Nuclear Engineering and Technology 51 (2019) 600–606

Contents lists available at ScienceDirect

Nuclear Engineering and Technology

journal homepage: www.elsevier.com/locate/net

Original Article

Large strain nonlinear model of lead rubber bearings for beyond design basis earthquakes

Seunghyun Eem*, Daegi Hahm

Structural and Seismic Safety Research Team, Korea Atomic Energy Research Institute, South Korea

ARTICLE INFO

Article history:
Received 20 July 2018
Received in revised form
21 October 2018
Accepted 2 November 2018
Available online 2 November 2018

Keywords:
Seismic isolation
Lead rubber bearing
Nonlinear numerical model
Isolation system
Nuclear power plants
Seismic response analysis

ABSTRACT

Studies on the application of the lead rubber bearing (LRB) isolation system to nuclear power plants are being carried out as one of the measures to improve seismic performance. Nuclear power plants with isolation systems require seismic probabilistic safety assessments, for which the seismic fragility of the structures, systems, and components needs be calculated, including for beyond design basis earthquakes. To this end, seismic response analyses are required, where it can be seen that the behaviors of the isolation system components govern the overall seismic response of an isolated plant. The numerical model of the LRB used in these seismic response analyses plays an important role, but in most cases, the extreme performance of the LRB has not been well studied. The current work therefore develops an extreme nonlinear numerical model that can express the seismic response of the LRB for beyond design basis earthquakes. A full-scale LRB was fabricated and dynamically tested with various input conditions, and test results confirmed that the developed numerical model better represents the behavior of the LRB over previous models. Subsequent seismic response analyses of isolated nuclear power plants using the model developed here are expected to provide more accurate results for seismic probabilistic safety assessments.

1. Introduction

To improve the seismic performance of nuclear power plants, ongoing studies are being carried out to apply seismic isolation systems [1–4]. Such systems work to provide separation between the structures and the ground to reduce loads from earthquakes using various isolation devices. As probabilistic safety assessments are commonly carried out to identify weaknesses in the design and operation of nuclear power plants [5], it is necessary to evaluate the effectiveness of any proposed safety enhancement measure, in this case the seismic isolation system, with a probabilistic safety assessment. In order to do this, information on the seismic fragilities of the plant's structures, systems, and components (SSCs) is needed, which in turn requires analyses of the seismic responses of the SSCs, including for beyond design basis earthquakes. Since the seismic responses of such superstructures and equipment are governed by the behavior of the isolation devices, a numerical model is needed to accurately analyze the response behavior of the SSCs for each seismic fragility analysis.

Three different isolation devices have been proposed for nuclear power plant isolation systems: the natural rubber bearing, the lead rubber bearing (LRB), and the friction bearing [6]. Among them, the LRB isolator consists of thin layers of alternating rubber and steel plates with a lead core, which results in a device structure that can withstand large vertical loading while maintaining an appropriate lateral stiffness [7]; this structure therefore provides for great energy absorption capacity during earthquake events [8]. Hence, the LRB is a promising isolation device to be applied in nuclear power plants. For design basis earthquakes, the strain of the LRB is expected to be 100–150% [9], while it is expected that this strain will increase by a factor of 3 in beyond design basis earthquakes [10]. The LRB shows explicit nonlinear behavior at large strain rates, which, based on experimental results, cannot be represented by simplified equivalent linear or bi-linear models.

Current numerical models of the LRB widely employ Bouc–Wen [11,12] and rate independent plasticity models [13]. Ioannis et al. [14] developed a model to express the strength degradation phenomenon of the LRB considering the effect of lead temperature, and Kumar et al. [15] developed one to express the shear behavior of the LRB considering the influence of vertical loading. Such numerical models have well established the shear behavior of the LRB in

* Corresponding author.
E-mail address: eemsh@kaeri.re.kr (S. Eem).

https://doi.org/10.1016/j.net.2018.11.001

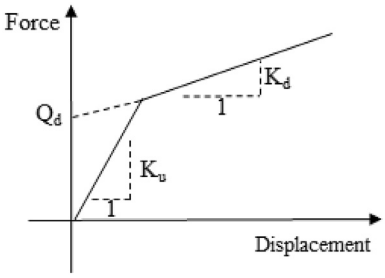

Fig. 1. Characteristics of the LRB isolator (bi-linear model): primary stiffness (K_1), second stiffness (K_2), and characteristic strength (Q_d).

Fig. 3. Set-up for the dynamic testing of the LRB.

Table 1
Lead rubber bearing isolator specifications.

	Value	Units
Inner diameter	320	mm
Outer diameter	1520	mm
Area of rubber	1.685	m^2
Area of lead	0.08	m^2
Total height of rubber	224	mm
Shear modulus of rubber	0.39	N/mm^2
Shear strength of lead	8.33	Mpa
Height of lead	441	mm

design basis earthquakes for regular structures. Although lateral displacement studies have been carried out by Kumar [15], there is a lack of research on the behavior of the LRB in beyond design basis earthquakes. In such conditions, the LRB experiences the hardening phenomenon, which is important in the calculation of the floor response spectrum of an isolated nuclear power plant [16]. In one numerical model for seismic isolation systems, Grant et al. [14,17] demonstrated the shear behavior of high-damping rubber bearings, which well-expresses the hardening phenomenon of the rubber under large displacement, but lacks adaptability to various input loads.

In order to evaluate the seismic risk of isolated nuclear power plants, it is necessary to develop an extreme nonlinear numerical model to analyze the ultimate behavior of the LRB for accurate seismic response analyses. In this study, an extreme nonlinear numerical model is developed that expresses the behavior of the LRB in a beyond design basis earthquake. First, dynamic testing of a full-scale LRB device (of about 1.5 m in diameter) subjected to various input conditions was conducted. To best express the identified characteristics of the LRB—namely, bi-linear behavior, hardening effect, and strength degradation—existing isolator numerical models were combined and optimized parameters found. This developed extreme nonlinear numerical LRB model, compared with the previous numerical models, better expresses the dynamic characteristics of the LRB device.

2. Dynamic testing of the lead rubber bearing

The behavior of the LRB is difficult to predict due to the high nonlinearity of its material characteristics; therefore, to understand the behavior of the LRB in an earthquake, dynamic tests must be conducted. First though, the related seismic isolation system has to be designed before the LRB can be fabricated for testing. The isolation system considered in this work was designed for the nuclear island of the APR-1400, which is a standard Korean nuclear power plant. The total weight of the APR-1400 nuclear island is 465,400 tons, and the target period of the isolation system is 2.41 s [18]. The design of the seismic isolation system usually determines the LRB's primary stiffness (K_1), secondary stiffness (K_2), and characteristic strength (Q_d), as shown in Fig. 1. These parameters are 49.71 kN/mm, 3.314 kN/mm, and 669.94 kN, respectively, for the present case (APR-1400), as defined by design code ASCE 4 for nuclear power plants. Using these values, the design parameters of the LRB device are defined and listed in Table 1, with a device schematic and picture shown in Fig. 2. The LRB isolation device tested here is a real-size bearing, which is relatively large compared with other research.

Dynamic testing of the LRB isolation device was performed in the Caltrans seismic response modification device (SRMD) test facility located at the University of California, San Diego [19]. The test

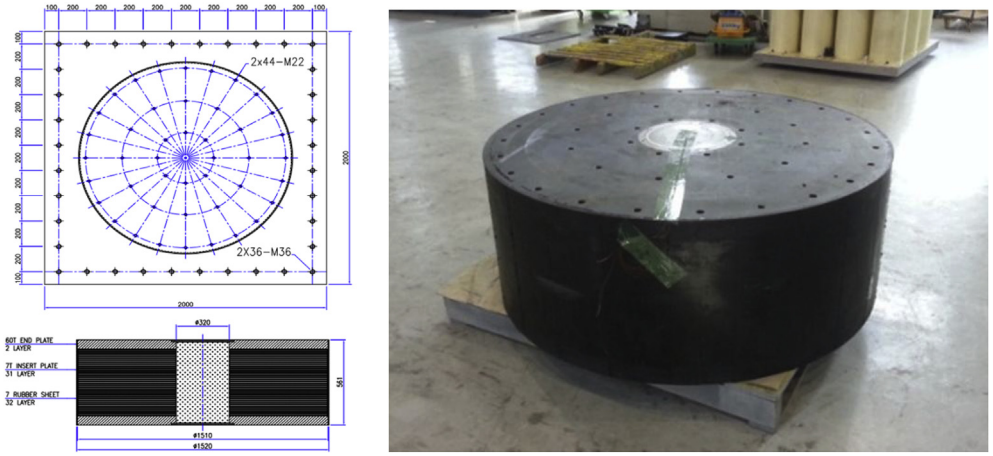

Fig. 2. (a) Schematics of the lead rubber bearing. (b) Manufactured LRB isolator.

Table 2
Dynamic test cases.

Test case	Disp. (mm)	Max. vel. (mm/s)	Load shape	Ver. load (kN)	Freq. (Hz)	# cycles	Shear strain (%)
1	224	14	SIN	22000	0.01	10	100
2	224	281	SIN	22000	0.2	10	100
3	224	704	SIN	22000	0.5	5	100
4	224	286	EQ	22000	–	–	–
5	448	563	SIN	22000	0.2	5	200
6	448	571	EQ	22000	–	–	–
7	672	844	SIN	22000	0.2	1	300
8	896	1126	SIN	22000	0.2	1	400

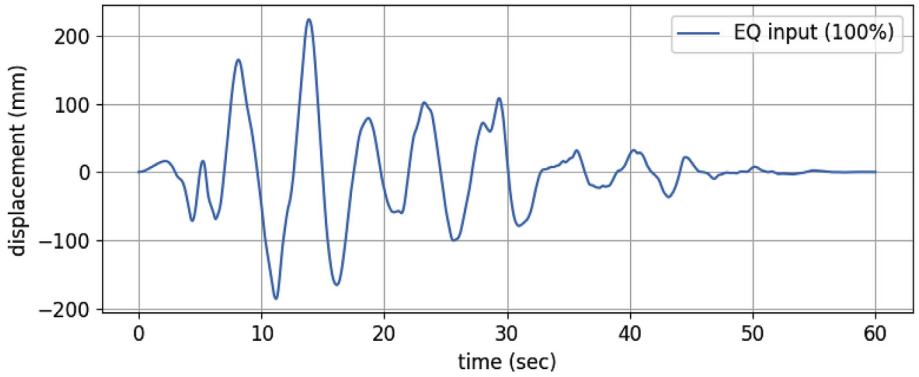

Fig. 4. Earthquake input for maximum shear strain 100% (test case 4).

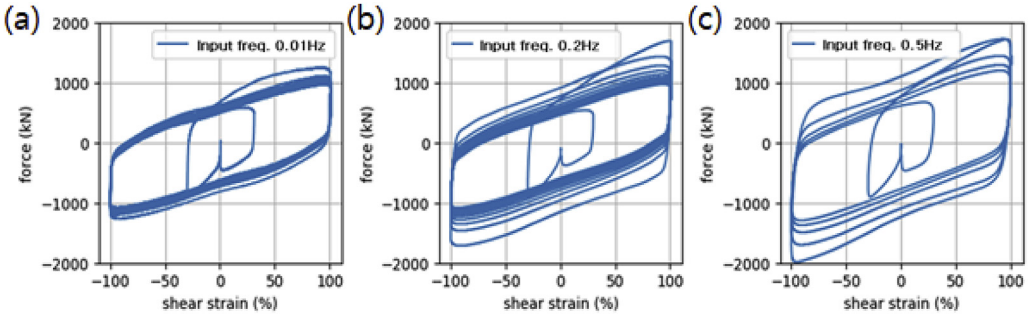

Figure 5. 100% shear strain test results with different input frequencies for test cases (a) 1, (b) 2, and (c) 3.

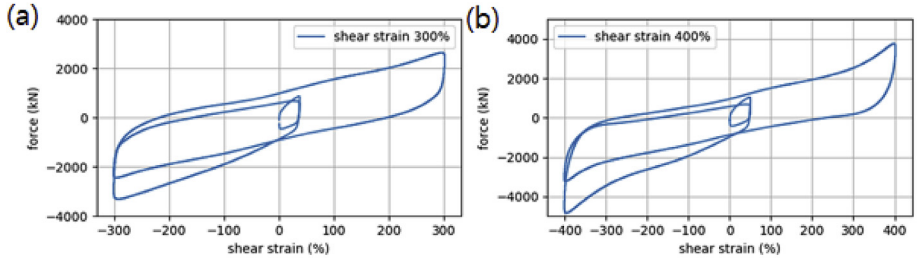

Figure 6. (a) 300% and (b) 400% shear strain test results (test cases 7 & 8).

rig allows for a real-time 6-DOF dynamic characterization of SRMDs. An overview of the set-up for the dynamic testing is depicted in Fig. 3; the LRB is fixed to the shaking table while the upper platen moves to apply loading.

In order to determine the dynamic behavior of the LRB device, eight test cases were conducted, as shown in Table 2. Dynamic testing was performed in a uniaxial direction by varying the displacement of the shaking table, with the movement and load of the shaking table measured. A shear strain of 100% here refers to a lateral movement of the device equaling the height of the rubber. Testing was divided into harmonic load s and seismic testings, designated as SIN and EQ in Table 2, respectively. For seismic testing (cases 4 and 6), the relative displacement of the LRB device was extracted and input to the shaking table based on the results of a seismic analysis of the related isolated nuclear power plant. The input motion for test case 4 is shown in Fig. 4.

Table 3
Parameters for the developed numerical model for the LRB.

Isolator Model	Parameter	Note
LeadRubberX	F_y	Yield strength
	α	Post-yield stiffness ratio
	G_r	Shear modulus of elastomeric bearing
	k_{bulk}	Bulk modulus of rubber
HDR	a_1 a_2 a_3 b_1 b_2 b_3	Parameters of the Grant model
IMK	K_0	Elastic stiffness
	as_Plus	Strain hardening ratio for positive loading direction
	My_plus	Effective yield strength for positive loading direction
	λ_S	Cyclic deterioration parameter for strength deterioration
	λ_C	Cyclic deterioration parameter for post-capping strength deterioration
	C_S	Rate of strength deterioration
	C_C	Rate of post-capping strength deterioration

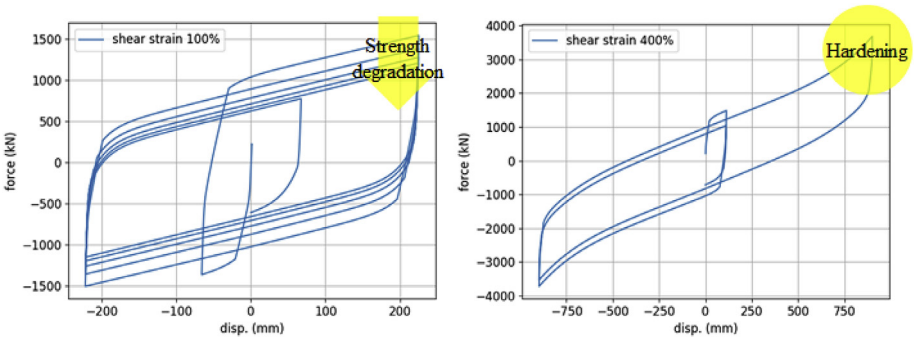

Fig. 7. Developed numerical model for the LRB isolator at shear strains of (a) 100% and (b) 400%.

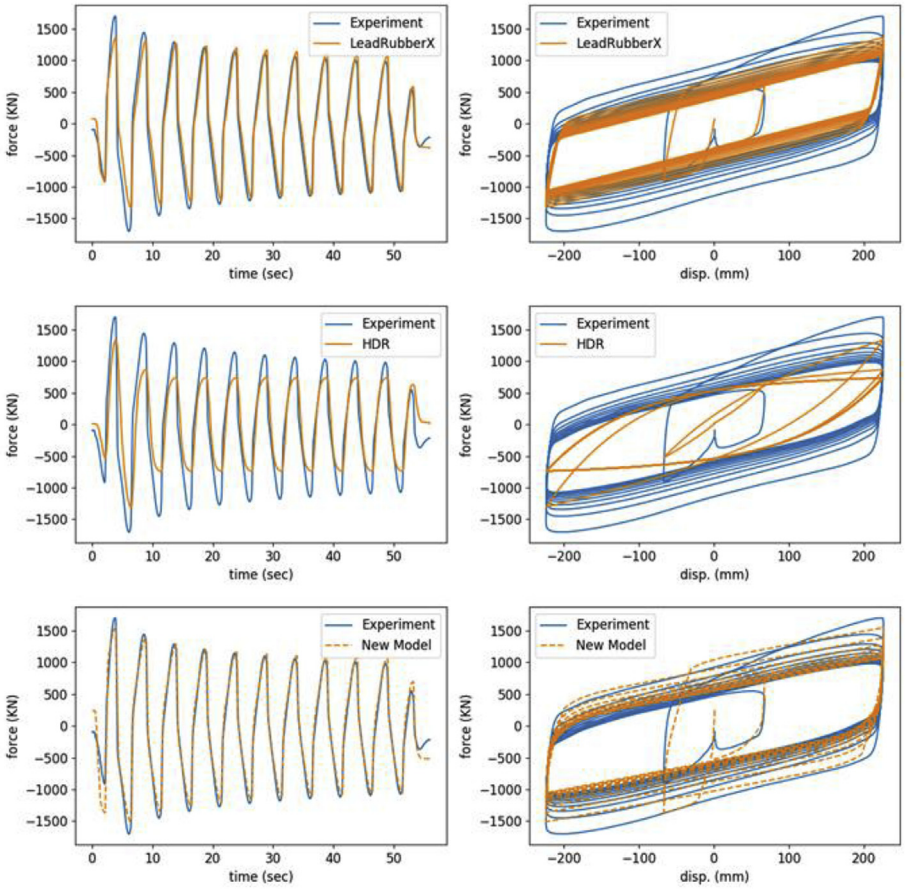

Fig. 8. Comparison between models and experiment for test case 2 (100% shear strain).

Fig. 5 shows the results for the 100% shear strain tests (cases 1–3). The bi-linear phenomenon, which is the basic characteristic of the LRB device, can be confirmed. Also, even at the same 100% shear strain, it is shown that the behavior differs according to the excitation frequency; as the excitation frequency increases, strength degradation also increases.

Seismic probabilistic safety assessments of isolated nuclear power plants require numerical models of the LRB isolation system that can express its behavior even for beyond design basis earthquakes. To this end, dynamic tests were carried out for a shear strain of more than 100%. Results show that the hardening phenomenon occurs between 250% and 300% of the shear strain of the LRB device (Fig. 6).

Dynamic testing of the isolation device confirmed the bi-linear, strength degradation, and hardening behaviors. As these three behaviors affect the floor response spectrum of the nuclear power plant, a numerical model of the LRB device that can represent the above phenomena should be developed for more accurate seismic response analysis results.

3. Extreme nonlinear numerical model of the lead rubber bearing

Numerical models of seismic isolation to be used for isolated nuclear power plants should be verified through dynamic testing of the related devices [20]. In the case of the LRB, the numerical model should well describe its nonlinear characteristics. Results of this study's dynamic testing not only confirmed the bi-linear characteristic of the LRB but also its hardening and strength degradation phenomena, characteristics that should be expressed in the new numerical model.

To represent the bi-linear, strength degradation, and hardening of the LRB device, a new model was developed by combining existing numerical models. The Opensees program was used for numerical analysis, with specific models LeadRubberX, high-damping rubber (HDR), and Ibarra–Medina–Krawinkler (IMK) employed to describe the LRB device. Among them, the LeadRubberX model basically utilizes the Bouc–Wen model and can express the behavior of an isolation device considering the effects of vertical load and temperature [21]. This model is based on material properties such as yield strength, post-yield stiffness ratio, shear modulus of elastomeric bearing, and bulk modulus of the rubber, as well as the geometric characteristics of internal diameter, outer diameter, steel and rubber layer thickness, and the number of rubber layers.

The HDR model was developed by Grant in 2004 to express the stiffness, damping, and degradation response of HDR bearings [17], and it was used here to represent hardening. The elastic component is obtained from a generalized Mooney–Rivlin strain energy function, and the hysteretic component is described by an approach similar to bounding surface plasticity. Degradation is separated into long- and short-term components [17]. Finally, the modified IMK deterioration model simulates the bi-linear hysteretic response. This model is a good representation of strength degradation in steel beam-to-column connections. These relationships were developed by Lignos and Krawinkler [21,22].

These three models were combined to cover the dynamic testing behaviors of the LRB. Particularly, LeadRubberX was used to

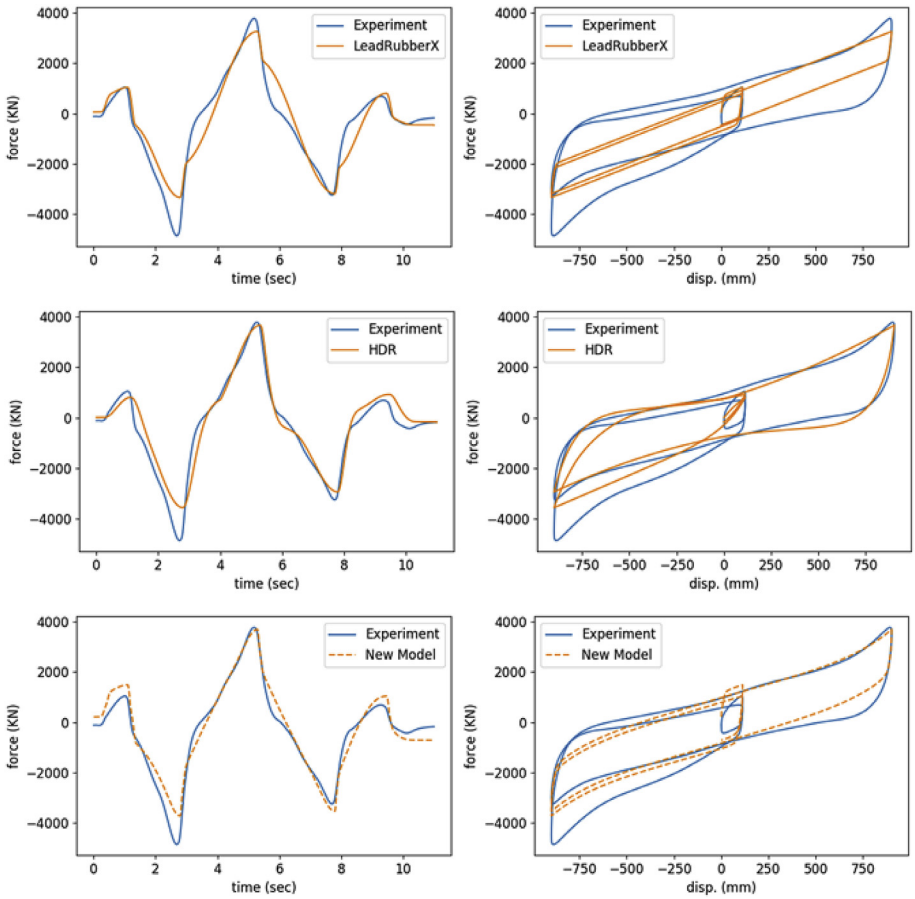

Fig. 9. Comparison between models and experiment for test case 8 (400% shear strain).

represent the bi-linear characteristic; it also describes the effects of temperature and vertical effects, but does not represent hardening or strength degradation. The HDR model well describes the nonlinear characteristics of isolation devices including hardening, but does not adequately describe the various behaviors of LRB devices under various loading conditions, which will be represented later. The IMK model well represents the strength degradation of the LRB. As a result, connecting these models in parallel can better reflect the dynamic test results of the LRB device. The coefficients of each model were found through an optimization technique, with the variables used for optimization in the combined model summarized in Table 3 below.

First, the design value was set to the initial value for optimization. Then, the coefficients of the LeadRubberX and IMK models for the main behavioral cycles of the LRB for strains where no hardening occurs (shear strain 100% harmonic load) were found. Coefficients of HDR were then found for the high shear-strain range where the hardening phenomenon occurs. While finding the coefficients for HDR, the coefficients of the LeadRubberX and IMK models were fixed. Fig. 7 shows the behavior of the developed numerical model for the LRB device, where it can be confirmed that the bi-linear characteristic is well represented. Strength degradation as the cycle increases can be seen in Fig. 7a, and hardening as the shear strain increases can be seen in Fig. 7b.

To verify its performance, results of the newly developed model were compared with those of previous LRB models as well as with the results of dynamic testing (Figs. 8–10). Optimal parameters were selected through the same dynamic test results and optimization method used for the LeadRubberX and HDR models. A Nelder–Mead optimization algorithm was used to determine the values for the coefficients (parameters) of the developed model [24]. The inputs for the optimization routine are the displacement and force of the shear deformation of the LRB isolator. The objective function is to minimize the difference between the measured force from the experiments and the predicted force from the developed model. The HDR model was mainly fitted to 400% shear strain, where the hardening effect is significant.

As can be seen in the figures, hardening is very well represented in HDR, but there is a difference from the test results for various loads. Likewise, LeadRubberX shows satisfactory results for 100% shear strain and seismic input, but it cannot express the hardening phenomenon well. On the other hand, the newly developed numerical model shows that bi-linear, hardening, and strength degradation characteristics are all well represented. In order to quantitatively compare the numerical model results with the dynamic testing results, fitness values are calculated in Eq. (1) [23]:

$$\text{fitness}\ (\%) = \left[1 - \frac{norm(F_{numerical\ model} - F_{experiment})}{norm(F_{experiment} - mean(F_{experiment}))}\right] \times 100. \quad (1)$$

Fitness values closer to 100% represent numerical model performance that better matches dynamic test results. Table 4 shows a comparison of the fitness values of each numerical LRB model. The average fitness value for the developed model is about 9% higher than the LeadRubberX model and about 25% higher than the HDR model. It can also be seen that the developed numerical model of

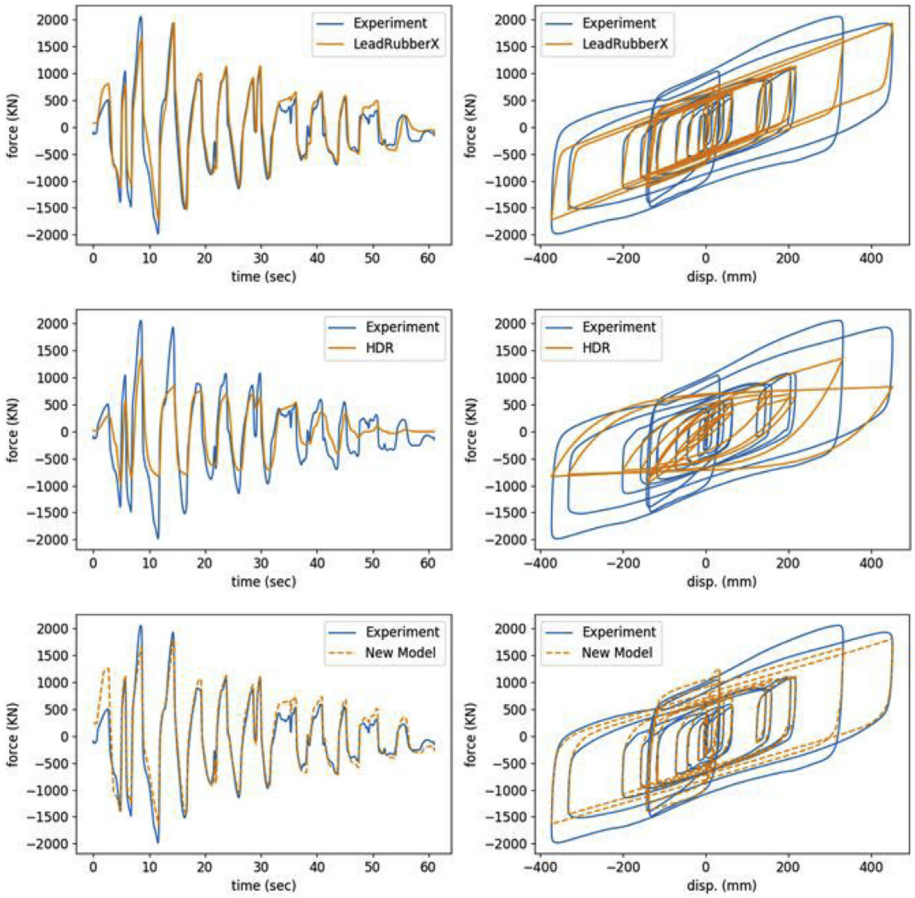

Fig. 10. Comparison between models and experiment for test case 6 (200% shear strain earthquake).

Table 4
The Fitness value of numerical model results with one optimal value set.

Test case	LeadRubberX	HDR	Developed Model
1	73.22	55.83	76.30
2	73.40	52.37	82.87
3	66.51	42.85	76.38
4	61.38	28.54	72.43
5	72.71	52.47	83.81
6	65.09	42.11	69.37
7	70.70	56.33	78.00
8	66.12	74.36	75.64
Average	68.64	50.60	76.85

the LRB isolator shows better results for a larger variety of input loads.

4. Conclusion

Seismic probabilistic safety assessments are needed to evaluate the seismic performance of isolated nuclear power plants, which require seismic response analyses, which in turn should include beyond design basis earthquakes. The isolation system dominates the seismic behavior of an isolated nuclear power plant; as the lead rubber bearing isolator is being considered for installation, numerical models of the LRB play an important role in seismic response analyses. Therefore, this study developed an accurate numerical model of the LRB to express its dynamic characteristics. A full-scale LRB device was fabricated, and dynamic testing was performed to understand the various characteristics of the isolation device, including shear strain of up to 400% to account for beyond design basis earthquakes. Testing confirmed the bi-linear, hardening, and strength degradation characteristics of the LRB. A numerical model of the LRB was then developed by combining existing numerical models of seismic isolation devices, with the new model reflecting the results of the dynamic tests and expressing the three characteristics well. The developed numerical model of the LRB was compared with previous numerical models of seismic isolation devices with various inputs, and it was confirmed that the dynamic behavior of the developed model outperforms previous numerical models.

This study was limited though considering that there are many parameters to be selected for comparison with other LRB numerical models. In order to express the hardening and strength degradation phenomena, parameters expressing the related behaviors should be selected through dynamic testing. While the model developed here can represent the 6-DOF behavior of the LRB, only its uniaxial behavior was verified in this paper. Therefore, future studies will use the developed model to study further 6-DOF LRB behaviors. Ultimately, seismic response analyses of isolated nuclear power plants using the developed model are expected to provide more accurate results for seismic fragility analyses, which will lead to more accurate estimates of seismic risk from seismic probabilistic safety assessment.

Acknowledgments

This work was supported by a National Research Foundation of Korea grant funded by the Korean government (NRF-2017M2A8A4014829).

Appendix A. Supplementary data

Supplementary data to this article can be found online at https://doi.org/10.1016/j.net.2018.11.001.

References

[1] S.H. Eem, H.J. Jung, Seismic response distribution estimation for isolated structures using stochastic response database, Earthquakes and Structures 9 (5) (2015) 937–956.
[2] A. Dusi, Seismic isolation of nuclear power plants, in: 15th World Conference on Earthquake Engineering, 2012.
[3] F. Perotti, M. Domaneschi, S. De Grandis, The numerical computation of seismic fragility of base-isolated Nuclear Power Plants buildings, Nucl. Eng. Des. 262 (2013) 189–200.
[4] A. Sarebanha, G. Mosqueda, M.K. Kim, J.H. Kim, Seismic response of base isolated nuclear power plants considering impact to moat walls, Nucl. Eng. Des. 328 (2018) 58–72.
[5] Korea Institute of Nuclear Safety, Safety review guides for PSR of PWRs, available online at: http://nsic.nssc.go.kr/htmlPdf/safetyReviewGuidesForPSRofPWRs.pdf, 2015. last accessed July 2018.
[6] ASCE. Seismic Analysis of Safety Related Nuclear Structures. ASCE STANDARD, 4-16.
[7] J.M. Kelly, D. Konstantinidis, Mechanics of Rubber Bearings for Seismic and Vibration Isolation, John Wiley & Sons, 2011.
[8] S.A. Mozaheb, F. Behnamfar, A new elastomeric-sliding seismic isolation system, Journal of Vibroengineering 20 (2) (2018) 1063–1074.
[9] I. Choi, J. Kim, M. Kim, Performance based design of LRB systems for nuclear power plants, in: Transactions, 24nd International Conference on Structural Mechanics in Reactor Technology (SMiRT-24), Busan, Korea, 2017.
[10] American Society of Civil Engineers, Seismic Analysis of Safety-related Nuclear Structures vols. 4–16, ACSE/SEI, USA, 2016.
[11] R. Bouc, Forced vibrations of mechanical systems with hysteresis, in: Proc. of the Fourth Conference on Nonlinear Oscillations, Prague, 1967, 1967.
[12] Y.K. Wen, Method for random vibration of hysteretic systems, J. Eng. Mech. Div. 102 (2) (1976) 249–263.
[13] S. Nagarajaiah, A.M. Reinhorn, M.C. Constantinou, Nonlinear dynamic analysis of 3-D-base-isolated structures, J. Struct. Eng. 117 (7) (1991) 2035–2054.
[14] I.V. Kalpakidis, M.C. Constantinou, A.S. Whittaker, Modeling strength degradation in lead–rubber bearings under earthquake shaking, Earthq. Eng. Struct. Dynam. 39 (13) (2010) 1533–1549.
[15] M. Kumar, A.S. Whittaker, M.C. Constantinou, An advanced numerical model of elastomeric seismic isolation bearings, Earthq. Eng. Struct. Dynam. 43 (13) (2014) 1955–1974.
[16] J.W. Jung, H.W. Jang, J.H. Kim, J.W. Hong, Effect of second hardening on floor response spectrum of a base-isolated nuclear power plant, Nucl. Eng. Des. 322 (2017) 138–147.
[17] D.N. Grant, G.L. Fenves, A.S. Whittaker, Bidirectional modelling of high-damping rubber bearings, J. Earthq. Eng. 8 (spec01) (2004) 161–185.
[18] S.H. Eem, H.J. Jung, Seismic fragility assessment of isolated structures by using stochastic response database, Earthquakes and Structures 14 (5) (2018) 389–398.
[19] G. Benzoni, D. Innamorato, G. Lomiento, N. Bonessio, KAERI BEARING TESTS BEARINGS 14L0110-14L0111 Tested April 2014(SRMD-2014-06), UCSD, La Jolla, CA, 2014.
[20] United States Nuclear Regulatory Commission (USNRC), (forthcoming). Technical Considerations for Seismic Isolation of Nuclear Facilities. NUREG, Washington DC.
[21] OpenSees, Open System for Earthquake Engineering Simulation, 2014. Version 2.4.4.
[22] D.G. Lignos, H. Krawinkler, Deterioration modeling of steel components in support of collapse prediction of steel moment frames under earthquake loading, J. Struct. Eng. 137 (11) (2010) 1291–1302.
[23] S.H. Eem, H.J. Jung, J.H. Koo, Modeling of magneto-rheological elastomers for harmonic shear deformation, IEEE Trans. Magn. 48 (11) (2012) 3080–3083.
[24] J.C. Lagarias, J.A. Reeds, M.H. Wright, P.E. Wright, Conver-gence properties of the Nelder-Mead simplex method in low dimensions, SIAM J. Optim. 9 (1998) 112–147.